Electron mobility in Gaussian heavily doped ZnO surface quantum wells

Doan Nhat Quang
Center for Theoretical Physics, Vietnamese Academy of Science and Technology, 10 Dao Tan Street, Hanoi, Vietnam

Le Tuan
Institute of Engineering Physics, Hanoi University of Technology, 1 Dai Co Viet Road, Hanoi, Vietnam

Nguyen Thanh Tien
College of Science, Can Tho University, 3-2 Road, Can Tho City, Vietnam

(Received 1 October 2007; revised manuscript received 13 February 2008; published 19 March 2008)

We present a theory of the low-temperature mobility of electrons in a Gaussian heavily doped zinc oxide surface quantum well (ZnO SFQW), taking into account both surface impurity and surface roughness scattering. The theory also includes strong confinement due to spontaneous polarization charges on the surface of ZnO. The electron distribution is found to be shifted closer to the surface for the O-polar face, while far away therefrom for the Zn-polar one. Accordingly, both scatterings are remarkably enhanced in the former case, while reduced in the latter one. Further, high-temperature Coulomb correlation among the charged impurities at a high density in a sample subjected to thermal treatment is proven to significantly reduce scattering by them. Therefore, in such a sample, surface roughness scattering dominates the electron mobility, while for a sample without thermal treatment, both scatterings are important. Our theory provides a good quantitative explanation of the experimental data on electron transport, in particular, the different carrier-density dependences of the mobilities measured in O-polar face ZnO SFQWs prepared in different ways, by bombardment with H_2^+ ions and by exposure to He^+ ions, which has not been explained so far.

DOI: 10.1103/PhysRevB.77.125326 PACS number(s): 73.50.Bk, 73.63.Hs

I. INTRODUCTION

In the last few years, zinc oxide (ZnO) has been intensively investigated because of its potential applications in ultraviolet and blue optoelectronic devices and its unique material properties, e.g., a wide band gap (3.37 eV) and a large exciton binding energy (60 meV).[1–4] In addition, it has a large variety of substrates, high transparency for visible light, and mixability with Mg and Cd to form a quaternary compound (Zn,Mg,Cd)O with a tunable band gap between 3.0 and 4.0 eV.[5]

It was experimentally indicated that accumulation layers, namely, two-dimensional electron gases (2DEGs), are formed at the naked surface of several semiconductors such as ZnO,[6–10] InP,[11] InGaAs,[12,13] SiGe,[14] and GaN.[15] This open structure is referred to as a surface quantum well (SFQW), in which a very high potential barrier between the vacuum and the host crystal leads to an enhanced electron confinement, i.e., a strong lateral quantization. An understanding of SFQWs is also important for the modeling of lateral quantization in other open systems, e.g., quantum wires and quantum dots. However, it should be mentioned that SFQWs have been much less studied than QWs, especially their electron transport, which is of importance for material characterization.

Among the above systems, the ZnO SFQW presents a great scientific interest. It allows a 2DEG of a surface density up to 5×10^{14} cm^{-2}, which is the highest value yet reported, more than an order of magnitude higher than that obtained in Si. In ZnO SFQWs, the ionized impurities (donors) of a so large density are located in the same space as the 2DEG (near to the surface). Thus, their influence on the 2DEG must be dramatic. Further, the many-body effects in the donor system and the electron one are clearly of importance. Indeed, the Coulomb repulsion between charged donors along the quantization direction gives rise to an inhomogeneous doping profile. For ion-implanted ZnO, the theoretical[16,17] and experimental[18,19] studies stipulate a Gaussian distribution for the impurities. This is distinct from the doping profiles explored extensively so far, where the impurity density is constant in the whole doping region.

It should be stressed that up to now, there have been few reports on the experimental data about the low-temperature electron mobility of ZnO SFQWs.[8–10] Moreover, no theoretical analysis is available. Therefore, the scattering processes limiting their electron transport remain unclear. As known, one of the ways to identify the key scattering mechanisms in a structure is to explore the dependence of its mobility on carrier density.

This functional dependence was measured for ZnO SFQWs of the O-polar face prepared differently, e.g., by bombardment with H_2^+ ions and by exposure to He^+ ions. It is worth mentioning that in the former case, the mobility shows a monotonic increase with a rise of the carrier density, whereas a maximum in the latter one. The interpretation of these different evolutions still is a challenge. Moreover, surface roughness scattering was ignored. This is implausible for ZnO SFQWs. Indeed, the quality of the naked surface of SFQWs is, in general, lower than that of buried interfaces in heterostructures.[17,20] Recent experimental studies provided evidence that the pure ZnO layer is rather rough.[21–23] Further, it was pointed out[24–26] that ZnO in the natural (wurtzite) phase has a large spontaneous polarization (twice of that of GaN). This must exert some influence on electron transport in ZnO-based structures, however, scarcely studied. Recently, we have shown[27,28] that polarization charges on an

 ©2008 The American Physical Society

interface of GaN-based heterostructures may bring about a remarkable shift of the electronic distribution toward this interface, so an enhancement of surface roughness scattering. Thus, surface roughness scattering in ZnO SFQWs is expected to be violent.

Thus, the aim of this paper is to present a theory of the low-temperature mobility of electrons confined in Gaussian heavy-doped ZnO SFQWs, taking adequately into account scattering by surface impurities and by surface roughness. In particular, we examine the impact of lateral quantization due to spontaneous polarization on these scatterings. For illustration of the theory, we calculate the carrier-density dependence of the 2DEG mobility in ZnO SFQWs.

The paper is organized as follows. In Sec. II, we describe the 2DEG in a Gaussian-doped ZnO SFQW, involving many-body effects in the donor and electron systems. In Sec. III, the basic relations necessary for calculating the 2DEG mobility are supplied and the autocorrelation functions for surface impurity and surface roughness scatterings are derived. Numerical calculations are carried out in Sec. IV in comparison with experimental data. Lastly, a summary is given in Sec. V.

II. TWO-DIMENSIONAL ELECTRON GAS IN A GAUSSIAN-DOPED SURFACE QUANTUM WELL

A. Confining potentials in a Gaussian-doped surface quantum well

We first examine the distribution of electrons in a Gaussian heavily doped ZnO SFQW. The potential barrier between the vacuum and ZnO is very high ($V_0 \sim 5$ eV) so that the penetration of electrons into the vacuum is negligibly small (infinite-barrier model). The 2DEG in the lowest subband of a ZnO SFQW is then described by a standard Fang–Howard wave function,[29]

$$\zeta(z) = (k^3/2)^{1/2} z e^{-kz/2}, \tag{1}$$

in ZnO ($z \geq 0$) and equal to zero in the vacuum ($z < 0$). Here, k is the wave number to be determined.

The quantum confinement along the z direction (normal to the surface) is determined by the following Hamiltonian:

$$H = T + V_{\text{tot}}(z), \tag{2}$$

where T is the kinetic energy and $V_{\text{tot}}(z)$ is the effective confining potential given by

$$V_{\text{tot}}(z) = V_b(z) + V_H(z) + V_p(z) + V_{\text{im}}(z) + V_{\text{xc}}(z). \tag{3}$$

All possible confining potentials are included and interpreted in what follows. The first term is due to a potential barrier located at the surface plane $z=0$,

$$V_b(z) = V_0 \theta(-z), \tag{4}$$

with $\theta(z)$ as a unity step function.

The second term is the Hartree potential due to the ionized donors and the confined electrons themselves. This is obtained from the Poisson equation,[30]

$$\frac{d^2}{dz^2} V_H(z) = \frac{4\pi e^2}{\varepsilon_L}[N_D(z) - n(z)], \tag{5}$$

where ε_L is the dielectric constant of ZnO and $N_D(z)$ and $n(z)$ are the bulk densities of ionized donors and electrons, respectively. The boundary conditions are such that $V_H(0)=0$ and $\partial V_H(\infty)/\partial z=0$.[29–31]

It was pointed out[16–19] that the donor density distribution in ZnO, especially under hydrogen-ion bombardment, is of Gaussian shape with a peak at some point $z_D > 0$ so that

$$N_D(z) = \frac{n_D}{\sigma\sqrt{2\pi}} \exp\left[-\left(\frac{z - z_D}{\sigma\sqrt{2}}\right)^2\right], \tag{6}$$

in ZnO and equal to zero in the vacuum. Here, σ is a standard deviation of the Gaussian function and the δ doping is its limiting case with $\sigma=0$.[32] The sheet density of donors is defined as

$$N_D^{2D} = \int_{-\infty}^{+\infty} dz N_D(z) = \frac{n_D}{2}\left[1 + \text{erf}\left(\frac{z_D}{\sigma\sqrt{2}}\right)\right], \tag{7}$$

where erf(x) and erfc(x) are the error and complementary error functions.[33]

The electron density distribution in ZnO is specified by the wave function from Eq. (1) as

$$n(z) = n_s |\zeta(z)|^2, \tag{8}$$

where n_s is a sheet density of electrons. Under overall charge neutrality, it holds

$$n_s = N_D^{2D}. \tag{9}$$

In this case, the sheet electron density is minimal for a Gaussian doping with the peak located at the surface ($z_D=0$) and maximal for δ doping ($\sigma=0$) so that $n_D/2 \leq n_s \leq n_D$.

As known,[34,35] we may solve the Poisson equation [Eq. (5)] with the above-quoted boundary conditions for the Hartree potential due to the whole charge system by separately integrating the Poisson equations for the donor subsystem and the 2DEG one with the same boundary conditions as for the Hartree potential. This means that for each charge subsystem, its potential at the surface ($z=0$) and its electric field in the bulk ($z \to \infty$) are vanishing. As a result, the Hartree potential may be derived as a sum of the two terms,

$$V_H(z) = V_D(z) + V_s(z), \tag{10}$$

where the partial potentials created by the donors and the confined electrons are, respectively, given by

$$V_D(z) = \frac{4\pi e^2}{\varepsilon_L}\frac{n_D\sigma}{\sqrt{2}}\left\{\frac{1}{\sqrt{\pi}}\exp\left[-\left(\frac{z-z_D}{\sigma\sqrt{2}}\right)^2\right] - \frac{1}{\sqrt{\pi}}\exp\left[-\left(\frac{z_D}{\sigma\sqrt{2}}\right)^2\right] + \frac{z-z_D}{\sigma\sqrt{2}}\text{erf}\left(\frac{z-z_D}{\sigma\sqrt{2}}\right) - \frac{z_D}{\sigma\sqrt{2}}\text{erf}\left(\frac{z_D}{\sigma\sqrt{2}}\right) - \frac{z}{\sigma\sqrt{2}}\right\} \tag{11}$$

and

$$V_s(z) = -\frac{4\pi e^2}{\varepsilon_L} n_s \left[\frac{e^{-kz}}{2k}(k^2z^2 + 4kz + 6) - \frac{3}{k} \right]. \quad (12)$$

The third term in Eq. (3) is the potential due to spontaneous polarization charges bound on the ZnO surface so that

$$V_p(z) = \frac{2\pi e^2(\sigma_p/e)}{\varepsilon_L} z, \quad (13)$$

with σ_p/e as their sheet density.

The fourth term is a classical repulsion potential due to image charge, which quantifies the effect arising from an abrupt decrease in the dielectric constant across the ZnO surface. This is yielded by[29,36]

$$V_{\rm im}(z) = \frac{\varepsilon_-}{\varepsilon_+} \frac{e^2}{\varepsilon_L} \frac{1}{4z}, \quad (14)$$

where by definition

$$\varepsilon_\pm = \frac{\varepsilon_L \pm 1}{2\varepsilon_L}, \quad \varepsilon_+ + \varepsilon_- = 1. \quad (15)$$

At last, the exchange-correlation corrections allow for the many-body effect in the 2DEG along the normal direction. In the literature, this was described by various models. Within a simple model, this is given by[37,34]

$$V_{\rm xc}(z) = -0.611 \frac{e^2}{\varepsilon_L} \left[\frac{3}{4\pi} n(z) \right]^{1/3}, \quad (16)$$

with $n(z)$ as the electron distribution from Eq. (8).

B. Total energy per electron in the lowest subband

Next, we turn to the total energy per particle in the ground-state subband, which is to be minimized to find the wave number k appearing in Eq. (1). Within the infinite-barrier model, the expectation value of the Hamiltonian from Eqs. (2), (3), and (10) is given by

$$E(k) = \langle T \rangle + \langle V_D \rangle + \langle V_s \rangle + \langle V_p \rangle + \langle V_{\rm im} \rangle + \langle V_{\rm xc} \rangle. \quad (17)$$

The total energy per electron is obtained by a modification of Eq. (17), in which the average 2DEG potential $\langle V_s \rangle$ is to be replaced with its half.[29]

Upon using the above-derived expressions for the partial confining potentials, we may estimate their expectations in the electron state with the wave function from Eq. (1). The average energies present in Eq. (17) are supplied in the following. For the kinetic energy, it holds

$$\langle T \rangle = \frac{\hbar^2 k^2}{8 m_z}, \quad (18)$$

where m_z is the out-of-plane effective electron mass of ZnO.

The average donor potential is given by

$$\langle V_D \rangle = \frac{4\pi e^2}{\varepsilon_L} \frac{n_D \sigma}{\sqrt{2}} \Bigg\{ \frac{a^3}{2\sqrt{2\pi}} e^{[(a-2\delta)^2/8]-\delta^2} D_{-3}\left(\frac{a-2\delta}{\sqrt{2}} \right) - \frac{a^3}{2} e^{-\delta a}[G_3(a,\delta) - 2\delta G_2(a,\delta) + \delta^2 G_1(a,\delta)] - \frac{3}{a} - \frac{1}{\sqrt{\pi}} e^{-\delta^2} - \delta\,{\rm erf}(\delta) \Bigg\}, \quad (19)$$

with the dimensionless variables defined by

$$a = k\sigma\sqrt{2} \quad \text{and} \quad \delta = \frac{z_D}{\sigma\sqrt{2}}. \quad (20)$$

Here, $D_l(x)$ is a parabolic cylinder function,[33] and we introduced an auxiliary function of two variables defined in terms of the error and complementary error functions,

$$G_l(x,\alpha) = \frac{\partial^l}{\partial x^l} \left\{ \frac{1}{x} \left[e^{\alpha x}\,{\rm erf}(-\alpha) + e^{x^2/4}\,{\rm erfc}\left(-\alpha + \frac{x}{2} \right) \right] \right\}, \quad (21)$$

with $l = 0, 1, 2, \ldots$ (integers).

The average 2DEG potential is

$$\langle V_s \rangle = \frac{33\pi e^2}{4\varepsilon_L} \frac{n_s}{k}. \quad (22)$$

The average polarization potential is

$$\langle V_p \rangle = \frac{2\pi e^2(\sigma_p/e)}{\varepsilon_L} \frac{3}{k}. \quad (23)$$

The average image potential is

$$\langle V_{\rm im} \rangle = \frac{\varepsilon_-}{\varepsilon_+} \frac{e^2}{\varepsilon_L} \frac{k}{8}. \quad (24)$$

At last, for the exchange-correlation corrections, it holds

$$\langle V_{\rm xc} \rangle = -0.611 \left(\frac{3}{4} \right)^4 \Gamma\left(\frac{11}{3} \right) \frac{e^2}{\varepsilon_L} \left(\frac{n_s k}{16\pi} \right)^{1/3}, \quad (25)$$

with $\Gamma(x)$ as a gamma function.[33]

III. LOW-TEMPERATURE ELECTRON MOBILITY

A. Basic equations

We are now dealing with quantum transport of electrons confined in a Gaussian heavily doped ZnO SFQW. At very low temperature, the mobility is determined via the transport lifetime τ by

$$\mu = e\tau/m^*, \quad (26)$$

with m^* as the in-plane effective electron mass of ZnO.

As known,[38,39] within the linear transport theory, the inverse transport lifetime is represented in terms of the autocorrelation function $\langle |U(q)|^2 \rangle$ for each scattering mechanism by

$$\frac{1}{\tau} = \frac{1}{2\pi\hbar E_F}\int_0^{2k_F} dq \frac{q^2}{(4k_F^2 - q^2)^{1/2}} \frac{\langle |U(q)|^2 \rangle}{\varepsilon^2(q)}, \quad (27)$$

where $q = 2k_F \sin(\vartheta/2)$ as the 2D momentum transfer by a scattering event in the x-y plane, with ϑ as a scattering angle. The Fermi energy is given by $E_F = \hbar^2 k_F^2 / 2m^*$, with $k_F = \sqrt{2\pi n_s}$ as the Fermi wave number.

The dielectric function $\varepsilon(q)$ entering in Eq. (27) takes account of the screening of scattering potentials by the 2DEG. As usual, this is evaluated within the random phase approximation,[29]

$$\varepsilon(q) = 1 + \frac{q_s}{q} F_S(q)[1 - G(q)] \quad \text{for } q \leqslant 2k_F, \quad (28)$$

where the inverse 2D Thomas–Fermi screening length is

$$q_s = \frac{2m^* e^2}{\varepsilon_L \varepsilon_+ \hbar^2}. \quad (29)$$

The screening form factor $F_S(q)$ takes account of the extension of electron states along the normal direction. For the wave function from Eq. (1), one has[29,36]

$$F_S(t) = \varepsilon_+ \frac{3at^2 + 9a^2 t + 8a^3}{8(t+a)^3} + \varepsilon_- \frac{a^6}{(t+a)^6}, \quad (30)$$

with $\varepsilon_\pm$ given by Eq. (15). Here, we introduced the dimensionless variables for the momentum transfer and the Fermi wave number,

$$t = q\sigma\sqrt{2} \quad \text{and} \quad t_F = k_F \sigma\sqrt{2}. \quad (31)$$

In Eq. (30), the first term ($\propto \varepsilon_+$) is connected with the Coulomb interaction between the electrons, while the second one ($\propto \varepsilon_-$) with that between them and their mirror images.

The local field corrections are due to a many-body exchange effect in the 2DEG in the in plane given by[40]

$$G(t) = \frac{t}{2(t^2 + t_F^2)^{1/2}}. \quad (32)$$

At very low temperature, the electrons in a ZnO SFQW are expected to experience the following scattering sources: surface impurities, i.e., ionized donors (IDs) and surface roughness (SR). The overall transport lifetime is determined by the ones for the partial scatterings according to the Matthiessen rule,

$$\frac{1}{\tau_{\text{tot}}} = \frac{1}{\tau_{ID}} + \frac{1}{\tau_{SR}}. \quad (33)$$

B. Autocorrelation functions for scattering mechanisms

1. Ionized donor

In accordance with Eqs. (26) and (27), for calculating the 2DEG mobility, we must derive the autocorrelation functions for the above scattering mechanisms. As known,[29] the autocorrelation function for scattering from a distribution of random (independent) ionized donors is given in terms of an integral over the doping region,

$$\langle |U_{ID}(q)|^2 \rangle = \left(\frac{2\pi e^2}{\varepsilon_L \varepsilon_+ q}\right)^2 \int_{-\infty}^{+\infty} dz_i N_D(z_i) F_R^2(q, z_i), \quad (34)$$

where $N_D(z_i)$ is the bulk donor density from Eq. (6). $F_R(q, z_i)$ denotes the form factor for a sheet of donors located in the plane $z = z_i$ and allows for the extension of electron states along the normal direction. Besides the donor position z_i, this also depends on the momentum transfer q.

For the wave function from Eq. (1), this is supplied in the ZnO region ($z_i > 0$) by[29]

$$F_R(t, z_i) = \varepsilon_+ P(t, z_i) + \varepsilon_- P_0(t, z_i), \quad (35)$$

where the first ($\propto \varepsilon_+$) and second ($\propto \varepsilon_-$) terms describe the scattering of 2DEG by the donors in the plane $z = z_i$ and by their mirror images, respectively. One of the functions entering in Eq. (35) is defined by

$$P_0(t, z_i) = \frac{a^3}{(t+a)^3} e^{-tz_i/\sigma\sqrt{2}}. \quad (36)$$

The other function is defined for two separate cases. For $t \neq a$,

$$P(t, z_i) = \frac{a^3}{(t-a)^3} \left\{ \left[u_1(t) + \frac{u_2(t)}{\sigma} z_i + \frac{u_3(t)}{2\sigma^2} z_i^2 \right] e^{-az_i/\sigma\sqrt{2}} - e^{-tz_i/\sigma\sqrt{2}} \right\}, \quad (37)$$

and for $t = a$,

$$P(t, z_i) = \frac{1}{8}\left[1 + \frac{\sqrt{2}a}{\sigma} z_i + \frac{a^2}{\sigma^2} z_i^2 + \frac{\sqrt{2}a^3}{3\sigma^3} z_i^3 \right] e^{-az_i/\sigma\sqrt{2}}, \quad (38)$$

where

$$u_1(t) = \frac{2t(t^2 + 3a^2)}{(t+a)^3}, \quad u_2(t) = -\frac{4at(t-a)}{\sqrt{2}(t+a)^2},$$

$$u_3(t) = \frac{t(t-a)^2}{t+a}. \quad (39)$$

Upon inserting Eqs. (35)–(38) into Eq. (34), we may represent the autocorrelation function for scattering by a Gaussian distribution of random donors in an analytic form,

$$\langle |U_{ID}(q)|^2 \rangle = \left(\frac{2\pi e^2}{\varepsilon_L \varepsilon_+}\right)^2 \sqrt{\frac{2}{\pi}} n_D \sigma^2 e^{-\delta^2} F_{ID}(t). \quad (40)$$

Here, the form factor $F_{ID}(t)$ is supplied below for two separate cases.

For $t \neq a$, it holds

$$F_{ID}(t) = \frac{a^6}{t^2}\left\{\left[\frac{\varepsilon_+^2}{(t-a)^6} - \frac{2\varepsilon_+\varepsilon_-}{(t^2-a^2)^3} + \frac{\varepsilon_-^2}{(t+a)^6}\right] \times e^{(t-\delta)^2/2} D_{-1}[\sqrt{2}(t-\delta)] - 2\left[\frac{\varepsilon_+^2}{(t-a)^6} - \frac{\varepsilon_+\varepsilon_-}{(t^2-a^2)^3}\right] \times e^{(t+a-2\delta)^2/8}\sum_{l=1}^{3} u_l(t) D_{-l}\left[\frac{t+a-2\delta}{\sqrt{2}}\right] + \frac{\varepsilon_+^2}{(t-a)^6} e^{(a-\delta)^2/2}\sum_{l=1}^{5} v_l(t) D_{-l}[\sqrt{2}(a-\delta)]\right\}, \quad (41)$$

where $D_l(x)$ are again parabolic cylinder functions and $v_l(t)$ are given in terms of the functions in Eq. (39) by

$$v_1(t) = u_1^2(t), \quad v_2(t) = 2u_1(t)u_2(t),$$

$$v_3(t) = 2[u_2^2(t) + u_1(t)u_3(t)],$$

$$v_4(t) = 6u_2(t)u_3(t), \quad v_5(t) = 6u_3^2(t). \quad (42)$$

For $t=a$, it holds

$$F_{ID}(t) = \frac{1}{64a^2} e^{(a-\delta)^2/2}\sum_{l=1}^{7} p_l(a) D_{-l}[\sqrt{2}(a-\delta)], \quad (43)$$

where $p_l(a)$ are powers of a given by

$$p_1(a) = 1, \quad p_2(a) = 2\sqrt{2}\varepsilon_+ a,$$

$$p_3(a) = 4\varepsilon_+(\varepsilon_+ + 1)a^2,$$

$$p_4(a) = 4\sqrt{2}\varepsilon_+(3\varepsilon_+ + 1)a^3, \quad p_5(a) = 56\varepsilon_+^2 a^4,$$

$$p_6(a) = 80\sqrt{2}\varepsilon_+^2 a^5, \quad p_7(a) = 160\varepsilon_+^2 a^6. \quad (44)$$

It should be mentioned that in the system under study, the doping level can be extremely high (up to $n_D \sim 5 \times 10^{14}$ cm^{-2}). Moreover, the sample is possibly subjected to thermal treatment (annealing), which enables the donors to diffuse. Therefore, the Coulomb repulsion between them becomes important.[32,41] Indeed, the interaction in question causes the donor distribution less random and reduces significantly the probability for large fluctuations in the donor density.[42,43] This implies that the donor correlation weakens scattering by them, so regarded as some screening (statistical). Their autocorrelation function is then diminished by a factor less than unity. We may write down

$$\langle |U_{ID}(q)|^2\rangle_c = \langle |U_{ID}(q)|^2\rangle F_C(q), \quad (45)$$

where the angular brackets with subindex c means the ensemble average over a correlated donor distribution. The correlation form factor is derived to be[43–45]

$$F_C(q) = \frac{q}{q+q_c}, \quad (46)$$

where q_c means the inverse Debye screening length of the donor gas at the diffusion freezing temperature (T_0) given by

$$q_c = \frac{2\pi e^2 N_D^{2D}}{\varepsilon_L \varepsilon_+ k_B T_0}, \quad (47)$$

with N_D^{2D} as the sheet donor density and k_B as the Boltzmann constant.

On substitution of Eq. (7) for the sheet donor density, we express the correlation form factor in terms of the dimensionless momentum transfer as follows:

$$F_C(t) = \frac{t}{t+t_c}, \quad (48)$$

with

$$t_c = \frac{\sqrt{2}\pi e^2 n_D \sigma}{\varepsilon_L \varepsilon_+ k_B T_0}\left[1 + \mathrm{erf}\left(\frac{z_D}{\sigma\sqrt{2}}\right)\right]. \quad (49)$$

It is seen from Eqs. (48) and (49) that the function of interest always exhibits a monotonic increase from zero to unity with an increase of the momentum transfer. This implies that the donor correlation suppresses scattering evens mainly with small momentum transfer ($t \sim 0$), i.e., forward scattering. In the literature another correlation form factor due to van Hall was sometimes used.[46–48] However, this seems to be unsatisfactory in view of the fact that in several cases this is nonmonotonic and greater than unity in some interval of the momentum transfer.

2. Surface roughness

It was pointed out[29] that the autocorrelation function for surface roughness scattering is fixed by the local value of the wave function at the surface. We have

$$U_{SR}(\mathbf{q}) = V_0|\zeta(0)|^2 \Delta_{\mathbf{q}}, \quad (50)$$

where $\Delta_{\mathbf{q}}$ denotes a Fourier transform of the surface roughness profile.

It is to be noticed that the right-hand side of Eq. (50) becomes indefinite in the limiting case of infinite potential barrier [$V_0 \to \infty$ and $\zeta(0) \to 0$]. Therefore, we need to adopt the following formula valid for any bound-state wave function,[29,36]

$$\int_{-\infty}^{+\infty} dz|\zeta(z)|^2 \frac{\partial V_{\mathrm{tot}}(z)}{\partial z} = 0, \quad (51)$$

which is exact and applicable for any value of the barrier height V_0. Upon replacing the effective confining potential with Eq. (3), we may represent the local value of the wave function in terms of the expectation values of the electric fields created by the partial confining sources,

$$V_0|\zeta(0)|^2 = \langle V_D'\rangle + \langle V_s'\rangle + \langle V_p'\rangle + \langle V_{\mathrm{im}}'\rangle + \langle V_{\mathrm{xc}}'\rangle, \quad (52)$$

with $V' = \partial V(z)/\partial z$.

Next, by putting Eq. (52) into Eq. (50), we arrive at the autocorrelation function for surface roughness,

$$\langle|U_{SR}(q)|^2\rangle = |\langle V_D'\rangle + \langle V_s'\rangle + \langle V_p'\rangle + \langle V_{\rm im}'\rangle + \langle V_{\rm xc}'\rangle|^2\langle|\Delta_{\mathbf{q}}|^2\rangle. \quad (53)$$

Thus, we must evaluate the average electric fields appearing in Eqs. (53). With the use of the wave function from Eq. (1), the result is given in the following.

For the Gaussian doping of a sheet donor density n_D,

$$\langle V_D'\rangle = -\frac{4\pi e^2}{\varepsilon_L}\frac{n_D}{2}\left\{1 - \frac{a^3}{2}e^{-\delta a}[G_2(a,\delta) - 2\delta G_1(a,\delta) + \delta^2 G_0(a,\delta)]\right\}. \quad (54)$$

For the 2DEG of a sheet density n_s,

$$\langle V_s'\rangle = \frac{4\pi e^2}{\varepsilon_L}\frac{n_s}{2}. \quad (55)$$

For polarization charges,

$$\langle V_p'\rangle = \frac{2\pi e^2(\sigma_p/e)}{\varepsilon_L}. \quad (56)$$

For the image potential,

$$\langle V_{\rm im}'\rangle = -\frac{\varepsilon_-}{\varepsilon_+}\frac{e^2}{\varepsilon_L}\frac{k^2}{8}. \quad (57)$$

Lastly, for exchange-correlation corrections,

$$\langle V_{\rm xc}'\rangle = -0.611\frac{9}{128}\left[2\Gamma\left(\frac{8}{3}\right) - \frac{3}{4}\Gamma\left(\frac{11}{3}\right)\right]\frac{e^2}{\varepsilon_L}\left(\frac{n_s k^4}{2\pi}\right)^{1/3}. \quad (58)$$

As seen from Eq. (53), surface roughness scattering is specified by the surface profile. This is normally written in the form

$$\langle|\Delta_{\mathbf{q}}|^2\rangle = \pi\Delta^2\Lambda^2 F_{SR}(t), \quad (59)$$

where Δ is a roughness amplitude, and Λ a correlation length. The roughness form factor is given by[49]

$$F_{SR}(t) = \frac{1}{(1+\lambda^2 t^2/4n)^{n+1}}, \quad (60)$$

where n is an exponent fixing its falloff at large momentum transfer t and $\lambda = \Lambda/\sigma\sqrt{2}$ is a reduced correlation length. For a rather rough ZnO surface, we will take a small exponent $n=1$. The correlation length Λ and roughness amplitude Δ are chosen as adjustable parameters for fitting to the experiment under study.

IV. RESULTS AND CONCLUSIONS

A. Validity of the model

In what follows, we will apply the foregoing theory to understand the transport properties of Gaussian heavily doped SFQWs formed near the surface of ZnO. First, we verify the validity of the above-adopted assumption of the existence of polar surfaces of ZnO. Following Tasker rules,[50] polar surfaces of ionic crystals should be generally unstable. However, ZnO is a notable exception since it has been confirmed by many experimental observations[51–57] that the nonreconstructed polar ZnO surfaces are stable. Their stabilization mechanisms are a subject under debate.

Moreover, there are various methods for producing accumulation layers on the free ZnO surface: (i) exposure to atomic hydrogen, (ii) illumination in vacuum by band-gap light, (iii) exposure to thermalized He^+ ions, and (iv) bombardment with H_2^+ ions. These methods may create strong accumulation layers; however, the polar ZnO surfaces are not damaged during the sample preparation.[8,10,17]

B. Material parameters

For numerical calculation, we need to specify the material parameters as input. For ZnO the dielectric constant is $\varepsilon_L = 8.2$,[58] and its diffusion freezing temperature T_0 is taken to be of the order of the annealing one.

In the natural phase ZnO has a large spontaneous polarization ($\sigma_p = -0.057$ C m^{-2}).[24,25] For the O-polar $(000\bar{1})$ face, this causes an attraction of electrons by a positive charge sheet density bound on the surface as high as $\sigma_p/e = 3.6 \times 10^{13}$ cm^{-2}, while for the Zn-polar (0001) face, a repulsion of them far away therefrom by a negative charge one of the same magnitude.

As known, the out-of-plane effective electron mass of ZnO is given as $m_z = 0.28\ m_e$,[59] whereas the in-plane one depends on the carrier density owing to nonparabolicity of the conduction band at large energies. So far, the experimental data of interest have been scarce in the literature. Therefore, we adopt an empirical approach based on a modified two-band model.[60,61] The in-plane effective electron mass at the ground-state energy varies as

$$m^* = m_0^*\left[1 + 2\beta\frac{\langle T\rangle + E_F}{E_g}\right], \quad (61)$$

where $m_0^* = 0.28\ m_e$ is its value at the band edge and $E_g = 3.37$ eV is the band-gap energy of ZnO. The carrier density dependence is specified via the Fermi energy $E_F = \pi\hbar^2 n_s/m^*$ and the average kinetic energy $\langle T\rangle$ in Eq. (18). The coefficient β allows for the multiband effect, namely, $\beta=1$ for the two-band Kane model with a nonparabolicity parameter equal to $1/E_g = 0.29$ eV^{-1},[2,62,63] and $\beta>1$ for higher-band contribution. In view of the fact that ZnO in the natural phase is similar in many respects to wurtzite GaN, we are to take the coefficient of the latter:[61] $\beta=2.5$ as a typical one for the former. Equation (61) is then equivalent to the two-band Kane model with a nonparabolicity parameter nearly equal to the mean value of those reported in Refs. 64 and 65.

The in-plane effective electron mass of ZnO is plotted in Fig. 1 and shows an increase with the sheet carrier density. Therefrom, we get $m^* = 0.5\ m_e$ at $n_s = 10^{14}$ cm^{-2}. This seems likely in agreement with the report:[2,65] $m^* \approx 0.5 m_e$ in the region $n_s > 2\times 10^{13}$ cm^{-2}, which was inferred from a measured carrier-density dependence of the plasma frequency in Al-doped ZnO.[65]

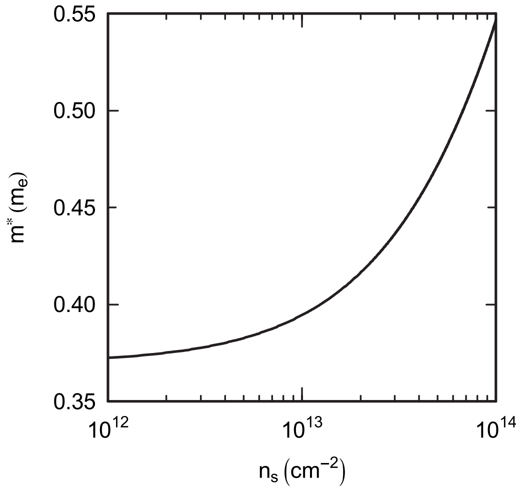

FIG. 1. In-plane effective electron mass of ZnO m^* vs sheet electron density n_s.

C. Effect of spontaneous polarization on the two-dimensional electron gas in ZnO surface quantum wells

We are concerned with the influence from spontaneous polarization on the 2DEG in Gaussian-doped ZnO SFQWs. We first examine the effect on quantum confinement. In Fig. 2, we display, following Eqs. (1), (8), and (9), the bulk electron density distribution $n(z)$ along the normal direction in the absence and the presence of spontaneous polarization for the O-polar and Zn-polar faces. The doping is specified with a high density $n_D = 10^{14}$ cm^{-2}, a standard deviation $\sigma = 12$ Å, and a peak position $z_D = 7$ Å.[17] There, the Gaussian bulk donor density distribution $N_D(z)$ is also sketched following Eq. (6).

Next, we evaluate the effect on the mobility determined by Eqs. (26) and (27) for the scattering mechanisms of interest for the 2DEG in ZnO SFQWs Gaussian doped with the same doping dimensions, as in Fig. 2, viz., $\sigma = 12$ Å and $z_D = 7$ Å, but the donor density n_D is varying with the sheet electron density n_s according to the charge neutrality. The mobility limited by ionized donors μ_{ID} as a function of electron density n_s is plotted in Fig. 3 for their random distribution by using Eqs. (40), (41), and (43) as well as for their correlated distribution by Eqs. (45), (48), and (49). In Fig. 4, the mobility limited by surface roughness μ_{SR} for the ZnO

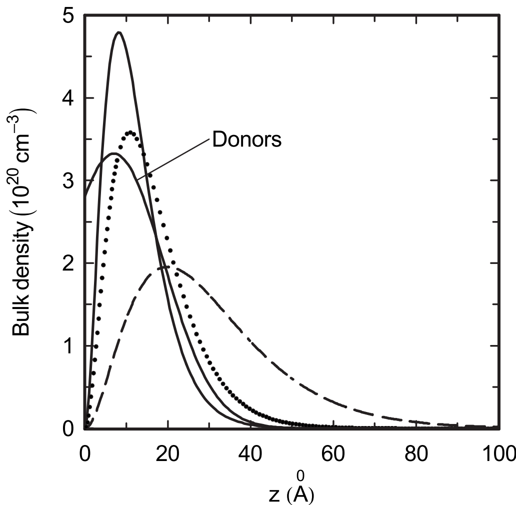

FIG. 2. Bulk density distribution $n(z)$ from the surface at $z=0$ along the normal direction for the 2DEG in a ZnO SFQW Gaussian doped with a density $n_D = 10^{14}$ cm^{-2}, a standard deviation $\sigma = 12$ Å, and a peak position $z_D = 7$ Å. The electron density distribution is displayed without (dotted line) and with spontaneous polarization for the O-polar face (solid line) and Zn-polar face (dashed one). The bulk donor density $N_D(z)$ is also shown (solid line).

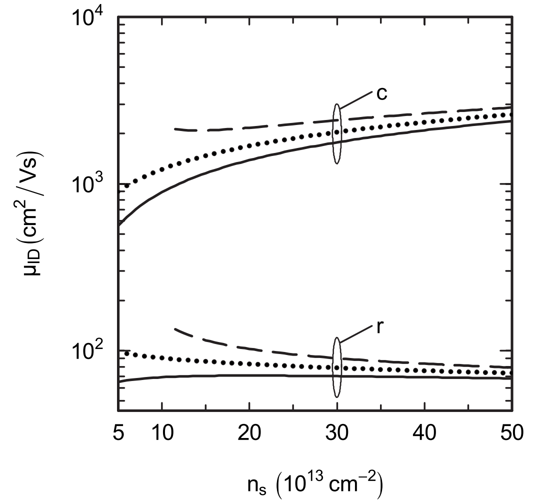

FIG. 3. Mobility limited by ionized donors μ_{ID} of the 2DEG in a ZnO SFQW Gaussian doped with the same doping dimensions as in Fig. 2 ($\sigma = 12$ Å and $z_D = 7$ Å) vs sheet electron density n_s in the absence (dotted lines) and the presence of spontaneous polarization for the O-polar face (solid lines) and Zn-polar face (dashed ones). The labels r and c refer to the random and correlated donor distributions, respectively.

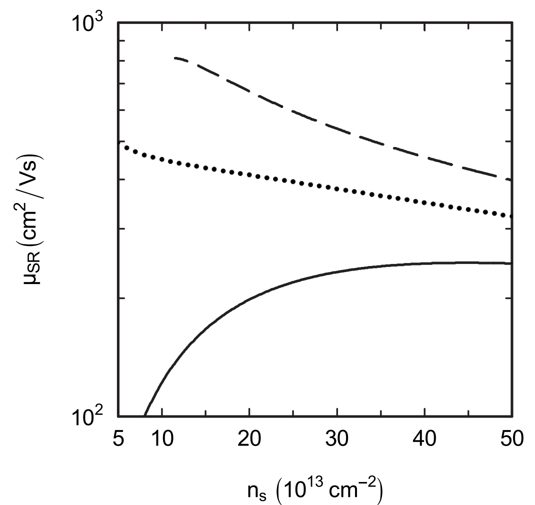

FIG. 4. Mobility limited by surface roughness μ_{SR} of the 2DEG in a ZnO SFQW Gaussian doped with the same doping dimensions as in Fig. 2 ($\sigma = 12$ Å and $z_D = 7$ Å) vs sheet electron density n_s in the absence (dotted line) and the presence of spontaneous polarization for the O-polar face (solid line) and Zn-polar face (dashed one). The surface profile is with an exponent $n = 1$, a roughness amplitude $\Delta = 10$ Å, and correlation length $\Lambda = 30$ Å.

SFQWs in Fig. 2 is plotted versus electron density n_s by using Eqs. (53)–(60). The surface profile is with an exponent $n=1$, a roughness amplitude $\Delta=10$ Å, and correlation length $\Lambda=30$ Å.

From Figs. 2–4, we may draw the following conclusions.

(i) It is clearly seen from Fig. 2 that the electron distribution in ZnO SFQWs depends drastically on spontaneous polarization. The 2DEG is to be shifted toward the surface and its peak is raised in a sample of O-polar face, whereas it shifted far away therefrom and its peak is reduced in a sample of Zn-polar face. As a result, the overlap between the electron and donor distributions is increased in the former case, but decreased in the latter one.

(ii) An inspection of Fig. 3 reveals that spontaneous polarization leads to a decrease of the donor-limited mobility in the O-polar face sample but an increase in the Zn-polar one. This is connected with, as mentioned above, an increase in overlapping between electron and donor distributions in the former case and a decrease in the latter one. The effect is somewhat larger than that in a modulation-doped sample, where the electrons and donors are separated in space, so the polarization effect on impurity scattering is weaker.[27]

(iii) Figure 4 indicates a similar effect of spontaneous polarization on the mobility limited by surface roughness. This is connected with the shift of the electron distribution toward the surface for the O-polar face sample and in the opposite direction for the Zn-polar face one. This means that the accumulation layer of O-polar face is of lower quality than that of Zn-polar one.

It is observed from Figs. 3 and 4 that the polarization effect on both scattering mechanisms is decreased with a rise of the electron density. In addition, the effect on surface roughness scattering is much larger than that on surface impurity one. As an example, the surface roughness mobility in an O-polar face sample is decreased by factor of 5 compared to the corresponding nonpolar face one at sheet electron densities $n_s \lesssim 5\times10^{13}$ cm^{-2}.

(iv) A comparison of the corresponding lines in Fig. 3 for the random and correlated distributions of impurities shows that the ionic correlation may remarkably increase the mobility limited by them, i.e., weaken the relevant scattering events. The increase may be of more than 1 order of magnitude at electron densities of $n_s \gtrsim 5\times10^{14}$ cm^{-2}, i.e., at extremely high doping levels.

D. Numerical results and comparison with experiment

To end this section, we apply the foregoing theory to explain the experimental data about the carrier-density dependence of the 2DEG mobility in O-polar face ZnO SFQWs. We are dealing with the samples prepared by bombardment of the O-polar face by 100 eV H_2^+ ions with subsequent thermal treatment (annealing at $T_0=700$ K)[10] and by exposure of the O-polar face to He^+ ions without thermal treatment (keeping below 100 K).[8] The ZnO SFQWs thus obtained were observed[10] to be different. The 2DEG created by H_2^+-ion implantation is practically inert to the surrounding ambient, while the one created by He^+-ion exposure is decayed by exposure to oxygen or air. Accordingly, the charge neutrality, Eq. (9), may hold in the former case, while be relaxed in the latter one.

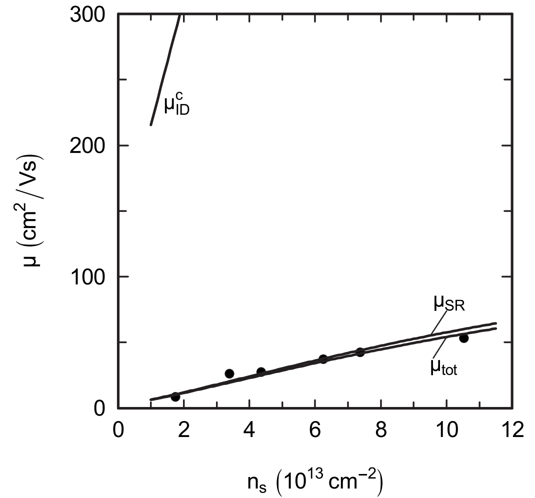

FIG. 5. Mobility of the 2DEG vs sheet electron density n_s in a ZnO SFQW prepared by bombardment of the O-polar face with 100-eV H_2^+ ions with subsequent thermal treatment as reported in Ref. 10. The partial mobilities are limited by ionized donors with correlation μ_{ID}^c, surface roughness μ_{SR}, and overall μ_{tot}. The experimental data marked by circles show a monotonic increase.

The calculated mobilities limited by ionized donors (μ_{ID}), surface roughness (μ_{SR}), and the overall mobility (μ_{tot}) are plotted versus electron density in Figs. 5 and 6, where the experimental data[8,10] are also reproduced for comparison. In Fig. 5, the result is displayed for the H_2^+-ion implanted sample reported in Ref. 10, where the Gaussian doping profile is for correlated donors with a standard deviation $\sigma=12$ Å and a donor peak position $z_D=7$ Å and the surface profile with a roughness amplitude $\Delta=13$ Å and a correlation length $\Lambda=26$ Å. The donor density n_D is varying with n_s

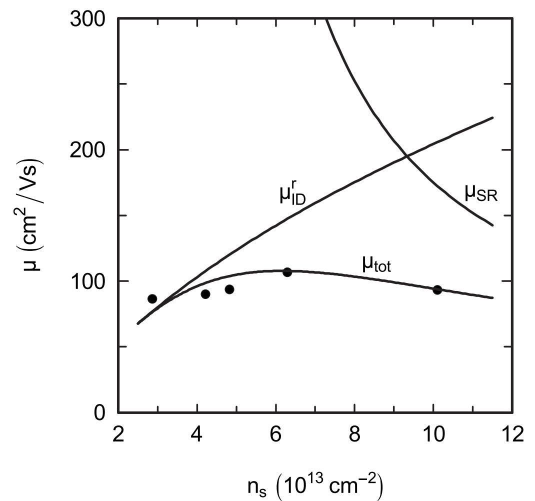

FIG. 6. Mobility of the 2DEG vs sheet electron density n_s in a ZnO SFQW prepared by exposure of the O-polar face to He^+ ions without thermal treatment, as reported in Ref. 8. The partial mobilities are limited by ionized donors without correlation μ_{ID}^r, surface roughness μ_{SR}, and overall μ_{tot}. The experimental data marked by circles exhibit a maximum.

according to the charge neutrality. In Fig. 6, the result is about the He^+-ion exposed sample reported in Ref. 8, where the doping profile is for uncorrelated donors with a density $n_D=10^{14}$ cm^{-2}, $\sigma=26$ Å, and $z_D=6$ Å, and the surface profile with $\Delta=6$ Å and $\Lambda=28$ Å.

It is noticed that the roughness amplitude in choice for the ZnO surface are somewhat large, e.g., compared to those for the Si and GaN ones. This is related to the poor quality of the ZnO surface as mentioned before.[21–23] In addition, the roughness amplitude of the H_2^+-ion implanted sample is larger as hydrogen doping may bring about an increase of surface roughness.[66,67]

From Figs. 5 and 6, we may draw the following conclusions.

(i) It is clearly seen from Figs. 5 and 6 that the overall mobilities calculated with inclusion of spontaneous polarization are in a good quantitative agreement with the carrier-density dependences measured in the diverse O-polar face ZnO SFQWs produced by both methods.

(ii) An inspection of Fig. 5 reveals that for the H_2^+-implanted ZnO SFQW the surface roughness scattering dominates the 2DEG mobility, while the impurity scattering is less relevant. The former is responsible for the increasing tendency of the mobility in the whole range of the carrier density in use.

(iii) It follows from Fig. 6 that for He^+-exposed ZnO SFQWs both scattering sources are important. The impurity scattering is responsible for the increasing tendency of the mobility at lower densities, while the surface roughness scattering for the decreasing tendency at higher densities. Both scattering mechanisms are combined, leading to the maximum detected experimentally.

V. SUMMARY

To summarize, in this paper, we have presented a comprehensive treatment of the low-temperature transport of the 2DEG in Gaussian heavily doped ZnO SFQWs. Our theory takes adequate account of the effect from large spontaneous polarization of ZnO on the electron distribution along the quantization direction and so on their mobility in the in plane.

It turns out that the quality of a ZnO accumulation layer depends strongly on its polarity. The large polarization charge bound on the ZnO surface causes a remarkable decrease in all partial mobilities of electrons in the O-polar face ZnO SFQW, whereas an increase in the Zn-polar face one.

We have pointed out that in ZnO SFQWs not only surface impurity but also surface roughness scattering play, in general, a key role. For the former mechanism, this is connected with a very high density of ionized donors, and for the latter one with a poor quality of the ZnO surface. In samples subjected to thermal treatment, the former scattering is significantly diminished, so that the latter one becomes dominant.

Our theory enables a good quantitative explanation of the different evolution of 2DEG mobility versus carrier density measured in samples prepared in different ways, by H_2^+-ion bombardment and by He^+-ion exposure.

Our theory is useful for the study of realistic δ-doped systems at high doping levels since the doping profile is of Gaussian rather than square form.[32,68]

[1] M. H. Huang, S. Mao, H. Feick, H. Yan, Y. Wu, H. Kind, E. Weber, R. Russo, and P. Yang, Science **292**, 1897 (2001).

[2] K. Ellmer, J. Phys. D **34**, 3097 (2001).

[3] D. C. Look, Semicond. Sci. Technol. **20**, S55 (2005).

[4] T. Makino, Y. Segawa, M. Kawasaki, and H. Koinuma, Semicond. Sci. Technol. **20**, S78 (2005).

[5] A. Ohtomo and A. Tsukazaki, Semicond. Sci. Technol. **20**, S1 (2005).

[6] Y. Goldstein and Y. Grinshpan, Phys. Rev. Lett. **39**, 953 (1977).

[7] D. Eger and Y. Goldstein, Phys. Rev. B **19**, 1089 (1979).

[8] Y. Grinshpan, M. Nitzan, and Y. Goldstein, Phys. Rev. B **19**, 1098 (1979).

[9] M. Nitzan, Y. Grinshpan, and Y. Goldstein, Phys. Rev. B **19**, 4107 (1979).

[10] G. Yaron, A. Many, and Y. Goldstein, J. Appl. Phys. **58**, 3508 (1985).

[11] R. M. Cohen, M. Kitamura, and Z. M. Fang, Appl. Phys. Lett. **50**, 1675 (1987).

[12] E. Yablonovitch, H. M. Cox, and T. J. Gmitter, Appl. Phys. Lett. **52**, 1002 (1988).

[13] J. Dreybrodt, A. Forchel, and J. P. Reithmaier, Phys. Rev. B **48**, 14741 (1993).

[14] K. Kishimoto, Y. Shiraki, and S. Fukatsu, Appl. Phys. Lett. **70**, 2837 (1997); Thin Solid Films **321**, 81 (1998).

[15] J. F. Muth, X. Zhang, A. Cai, D. Fothergill, J. C. Roberts, P. Rajagopal, J. W. Cook, Jr., E. L. Piner, and K. J. Linthicum, Appl. Phys. Lett. **87**, 192117 (2005).

[16] J. Lindhart, M. Scharff, and H. E. Schiott, K. Dan. Vidensk. Selsk. Mat. Fys. Medd. **33**, No. 14 (1963).

[17] V. Bogatu, A. Goldenblum, A. Many, and Y Goldstein, Phys. Status Solidi B **212**, 89 (1999).

[18] G. Yaron, J. Levy, Y. Goldstein, and A. Many, J. Appl. Phys. **59**, 1232 (1986).

[19] A. Many, Y. Goldstein, G. Yaron, and J. Levy, Surf. Sci. **170**, 416 (1986).

[20] D. Egger, A. Many, and Y. Goldstein, Phys. Lett. **55A**, 197 (1975).

[21] K. Grasza, E. Lusakowska, P. Skupinski, K. Kopalko, J. Bak-Misiuk, and A. Mycielski, Phys. Status Solidi B **244**, 1468 (2007).

[22] Y. B. Kwon, M. Abouzaid, P. Ruterana, and J. H. Je, Phys. Status Solidi B **244**, 1583 (2007).

[23] B. Y. Oh, M. C. Jeong, M. H. Ham, and J. M. Myoung, Semicond. Sci. Technol. **22**, 608 (2007).

[24] A. Dal Corso, M. Posternak, R. Resta, and A. Baldereschi, Phys. Rev. B **50**, 10715 (1994).

[25] F. Bernardini, V. Fiorentini, and D. Vanderbilt, Phys. Rev. B **56**, R10024 (1997).

[26] M. W. Allen, P. Miller, R. J. Reeves, and S. M. Durbin, Appl. Phys. Lett. **90**, 062104 (2007).
[27] D. N. Quang, V. N. Tuoc, N. H. Tung, N. V. Minh, and P. N. Phong, Phys. Rev. B **72**, 245303 (2005).
[28] D. N. Quang, N. H. Tung, V. N. Tuoc, N. V. Minh, H. A. Huy, and D. T. Hien, Phys. Rev. B **74**, 205312 (2006).
[29] T. Ando, A. B. Fowler, and F. Stern, Rev. Mod. Phys. **54**, 437 (1982).
[30] R. Enderlein and N. J. M. Horing, *Fundamentals of Semiconductor Physics and Devices* (World Scientific, Singapore, 1997).
[31] F. Stern, Phys. Rev. B **5**, 4891 (1972).
[32] E. F. Schubert, in *Semiconductors and Semimetals*, edited by A. C. Gossard (Academic, New York, 1994), Vol. 40, Chap. 1, p. 1.
[33] *Handbook of Mathematical Functions*, edited by M. Abramowitz and I. A. Stegun (Dover, New York, 1970).
[34] P. Ruden and G. H. Döhler, Phys. Rev. B **27**, 3538 (1983).
[35] G. Bastard, *Wave Mechanics Applied to Semiconductor Heterostructures* (Les Editions de Physique, Paris, 1988).
[36] T. Ando, J. Phys. Soc. Jpn. **43**, 1616 (1977).
[37] W. Kohn and L. J. Sham, Phys. Rev. **140**, A1133 (1965).
[38] F. Stern and W. E. Howard, Phys. Rev. **163**, 816 (1967).
[39] A. Gold, Phys. Rev. B **35**, 723 (1987).
[40] M. Jonson, J. Phys. C **9**, 3055 (1976).
[41] E. F. Schubert, J. E. Cunningham, and N. T. Tsang, Solid State Commun. **63**, 591 (1987).
[42] A. L. Efros, F. G. Pikus, and G. G. Samsonidze, Phys. Rev. B **41**, 8295 (1990).
[43] D. N. Quang, N. N. Dat, and D. V. An, Phys. Lett. A **182**, 125 (1993).
[44] D. N. Quang and N. H. Tung, Phys. Status Solidi B **207**, 111 (1998).
[45] O. Mezrin and A. Shik, Superlattices Microstruct. **10**, 107 (1991).
[46] P. J. van Hall, Superlattices Microstruct. **6**, 213 (1989).
[47] P. T. Coleridge, Phys. Rev. B **44**, 3793 (1991).
[48] B. Rössner, D. Chrastina, G. Isella, and H. von Känel, Appl. Phys. Lett. **84**, 3058 (2004).
[49] R. M. Feenstra and M. A. Lutz, J. Appl. Phys. **78**, 6091 (1995).
[50] P. W. Tasker, J. Phys. C **12**, 4977 (1979).
[51] S. H. Overbury, P. V. Radoluvic, S. Thevuthasan, G. S. Herman, M. A. Henderson, and C. H. F. Peden, Surf. Sci. **410**, 106 (1998).
[52] T. M. Parker, N. G. Condon, R. Lindsay, F. M. Leibsle, and G. Thornton, Surf. Sci. **415**, L1046 (1998).
[53] A. Wander, F. Schedin, P. Steadman, A. Norris, R. McGrath, T. S. Turner, G. Thornton, and N. M. Harrison, Phys. Rev. Lett. **86**, 3811 (2001).
[54] A. Wander and N. M. Harrison, J. Chem. Phys. **115**, 2312 (2001).
[55] O. Dulub, L. A. Boatner, and U. Diebold, Surf. Sci. **519**, 201 (2002).
[56] O. Dulub, U. Diebold, and G. Kresse, Phys. Rev. Lett. **90**, 016102 (2003).
[57] R. Lindsay, C. A. Muryn, E. Michelangeli, and G. Thorton, Surf. Sci. **565**, L283 (2004).
[58] T. Makino, A. Tsukazaki, A. Ohtomo, M. Kawasaki, and H. Koinuma, Jpn. J. Appl. Phys., Part 1 **45**, 6346 (2006).
[59] E. Mollwo, *Semiconductors: Physics of II–VI and I–VII Compounds, Semimagnetic Semiconductors*, Landolt-Börnstein, New Series, Vol. 17, edited by O. Madelung, M. Schulz, and H. Weiss (Springer, Berlin, 1982), p. 35.
[60] J. Singleton, R. J. Nicholas, D. C. Rogers, and C. T. B. Foxon, Surf. Sci. **196**, 429 (1988).
[61] S. Syed, J. B. Heroux, Y. J. Wang, M. J. Manfra, R. J. Molnar, and H. L. Stormer, Appl. Phys. Lett. **83**, 4553 (2003).
[62] W. Zawadzki, in *Handbook on Semiconductors*, edited by W. Paul (North-Holland, Amsterdam, 1982), Vol. 1, Chap. 12, p. 713.
[63] W. Knap, H. Alause, J. M. Bluet, J. Camassel, J. Young, M. Asif Khan, Q. Chen, S. Huant, and M. Shur, Solid State Commun. **99**, 195 (1996).
[64] T. Minami, H. Sato, K. Ohashi, T. Tomofuji, and S. Takata, J. Cryst. Growth **117**, 370 (1992).
[65] S. Brehme, F. Fenske, W. Fuhs, E. Neubauer, M. Poschenrieder, B. Selle, and I. Sieber, Thin Solid Films **342**, 167 (1999).
[66] S. Y. Myong and K. S. Lim, Appl. Phys. Lett. **82**, 3026 (2003).
[67] P. Sagar, M. Kumar, and R. M. Mehra, Thin Solid Films **489**, 94 (2005).
[68] P. M. Koenraad, F. A. P. Blom, C. J. G. M. Langerak, M. R. Leys, J. A. A. J. Perenboom, J. Singleton, S. J. R. M. Spermon, W. C. van der Vleuten, A. P. J. Voncken, and J. H. Wolter, Semicond. Sci. Technol. **5**, 861 (1990).